Journal of Applied Polymer Science

Matrix effect of mixed-matrix membrane containing CO_2-selective MOFs

Jiyoung Kim,[1] Jiyoung Choi,[1] Yong Soo Kang,[2] Jongok Won[1]

[1]Department of Chemistry, Sejong Polymer Research Center, Sejong University, 209, Neungdong-Ro, Gwangjin-Gu, Seoul 143-747, Korea

[2]Department of Energy Engineering, Hanyang University, 222 Wangsimni-Ro, Seongdong-Gu, Seoul 133-791, Korea

Correspondence to: J. Won (E-mail: jwon@sejong.ac.kr)

ABSTRACT: Facilitated mixed-matrix membranes (MMMs) containing Cu-metal organic frameworks (Cu-MOFs) with high CO_2 selectivity on an asymmetric polysulfone support were fabricated and examined the effect of gas separation performance using different matrices. An amorphous poly(2-ethyl-2-oxazoline) (POZ) and semicrystalline poly(amide-6-b-ethylene oxide) (PEBAX®MH 1657) block copolymer were chosen as the polymeric matrix and the effect of the matrix on CO_2 separation for MMMs containing Cu-MOFs was investigated. The interaction of CO_2 in different matrix was investigated theoretically using the density functional theory method, and it was found that the amide segment in PEBAX would contribute more to the CO_2 solubility than ether segment. The morphological changes were investigated by differential scanning calorimetry, field emission scanning electron microscope and X-ray diffractometer. The ideal selectivity of CO_2/N_2 was enhanced significantly with the addition of a Cu-MOF, and the values are higher in the Cu-MOF/PEBAX MMM compared with that in a POZ based asymmetric MMM. Improvement in the CO_2/N_2 selectivity of a Cu-MOF/PEBAX MMM was achieved via facilitated transport by the CO_2-selective Cu-MOFs due to both their high adsorption selectivity of CO_2 over N_2 and the decreased crystallinity of PEBAX due to the presence of the Cu-MOFs, which would provide a synergic effect on the CO_2 separation. © 2015 Wiley Periodicals, Inc. J. Appl. Polym. Sci. **2016**, *133*, 42853.

KEYWORDS: applications; membranes; porous materials; separation techniques; structure–property relations

Received 17 June 2015; accepted 20 August 2015

DOI: 10.1002/app.42853

INTRODUCTION

A polymeric separation membrane is considered to be an effective approach for the separation of gaseous mixtures due to the high separation efficiency and low operation cost compared with conventional separation methods.[1–4] However most of the polymeric membranes suffer from the trade-off between the permeability and the selectivity;[5] the selectivity decreases with increasing permeability. This trade-off in membrane performance can be overcome by adopting facilitated transport using a selective CO_2 carrier, and one candidate for the carrier is CO_2-selective metal-organic frameworks (MOFs). Because the permeability and selectivity properties can be manipulated in MOFs by the combination of metal ions and organic linkers during synthesis, it is possible to apply functional sites that have an interaction between the MOF and CO_2. If the interaction between the MOF and CO_2 could be optimized, facilitated transport membranes that contain a gas-selective MOF carrier would circumvent the trade-off.

With the development of tremendous nanoporous MOFs, several mixed-matrix membranes (MMMs) that contain a nanoporous MOFs in a polymer matrix have recently been reported.[6–15] However, most of studies are focused on the high porosity and structural selectivity of MOFs, which exhibit a molecular sieving ability with high permeability, rather than the selectivity. To adopt an advantage of porous MOFs into the facilitated transport membrane, a high selectivity of CO_2 and reversible interactions between CO_2 and the pore of the MOFs are necessary. We therefore prepared the CO_2-selective MOFs, $[\{Cu_2(Glu)_2(\mu\text{-bpa})\}\cdot(CH_3CN)]_n$ where bpa = 1,2-bis(4-pyridyl)ethane (Cu-MOFs),[16] which have a relatively high selectivity towards CO_2 over N_2 at room temperature.

The choice of the matrix polymer is important to fabricate MMMs containing Cu-MOFs. Although matching the MOF to the polymeric matrix is considered relatively easy than the one based on zeolite because of the partially organic segment of the MOFs, it is still difficult to obtain a perfect match between the polymer matrix and the MOF for the preparation of defect-free MMMs. If there are a non-selective voids resulting from the incompatibility between MOF materials and the polymer matrix at their interface and the pores are large enough for gas molecules to diffuse through them, the overall selectivity of the membrane will be reduced.

There are several surface modification approaches to enhance the interfacial adhesion between the MOF and the polymer matrix,[14,17] the resulting MMMs still suffer from low compatibility between these components, and most of the membrane exhibits improved permeability rather than selectivity. Recently preparation of MOF-MMMs by using particle fusion of polymer particles and the *in-situ* synthesized MOF particles.[18] Not to mention of these modification steps add to the cost and complexity of membrane fabrication and make such MMMs less competitive.[17,19]

As one way to solve this problem, we focused on the application of a CO_2-selective MOF as a carrier for the facilitated transport membrane. If the interactions between the MOF and CO_2 are high enough and reversible for the action of the CO_2 carrier, then it is possible to fabricate the highly selective asymmetric MMM, despite the poor structural selectivity resulting from the interfacial void between the polymer matrix and the MOF. Previously, two different gas-selective micro-sized frameworks were synthesized and dispersed in polyoxazoline (POZ), as a matrix for the fabrication of facilitated MMM.[20] It was found that the CO_2/N_2 selectivity of the membranes was improved via both high adsorption selectivity of CO_2 over N_2 by the Cu-MOFs, and the difference in pore sizes in the previous result.[20] Since POZ is a low-permeable and low-selective polymer, it is a good matrix to see the effect of the Cu-MOF as a carrier for CO_2, however, the CO_2 permeance was maintained at the same order of magnitude while the ideal selectivity of CO_2/N_2 increased significantly. To enhance the CO_2 permeance of Cu-MOF MMM while maintaining high selectivity, it is necessary to understand the role of the matrix in MMM containing CO_2 selective Cu-MOFs.

Because the Cu-MOFs are stable in ethanol, PEBAX®MH 1657 (PEBAX) is chosen as the polymeric matrix, which are dissolved in ethanol; ethanol is a good choice for the preserve the morphology of the polysulfone membrane support. PEBAX is a thermoplastic elastomer that has flexible polyether and rigid polyamide segments, which will provide a good CO_2 separation membrane which would provide a high selective MMM.[21–27]

Here, the MMM-containing Cu-MOF was prepared by casting the polymer solution containing different amounts of Cu-MOFs onto a commercial macroporous polysulfone membrane support. Because the permselectivity of a gas-separation membrane depends on the carrier and matrix, we focused our attention on the interaction between CO_2 and the matrix and the change of permselectivity with the addition of Cu-MOFs in both polymer matrices. The interaction of CO_2 in different matrix will be investigated theoretically using the density functional theory (DFT).[28,29] On the basis of the complexation energy, the difference in permselectivity due to the different matrices will be understood.

EXPERIMENTAL

Chemicals

Copper(II) nitrate trihydrate (99%), 1,2-bis(4-pyridyl)ethane (99%), acetonitrile (99.5%), polyoxazoline (POZ, Mw∼500,000), and acetone were purchased from Aldrich Chemical. PEBAX® MH 1657 was kindly provided by ARKEMA. Disodium glutarate (99%) was purchased from TCI. Methanol and ethanol were purchased from J.T.Baker. All of the solvents were analytical grade, and all of the chemicals were used without further purification. Cu-MOFs were synthesized as described elsewhere.[16] Disodium glutarate (0.0352 g, 0.02 mmol) and $Cu(NO_3)_2{\cdot}3H_2O$ (0.0242 g, 0.1 mmol) were dissolved separately in 20 mL of H_2O. These solutions were mixed with 20 mL of 1,2-bis(4-pyridyl ethane) methanol solution (0.0368 g, 0.2 mmol). Solutions were mixed in a glass bottle, which was capped and stored at room temperature for 24 h. After the reaction, a green powder was collected by centrifugation, washed several times with water and ethanol, and dried under vacuum at room temperature before being used in the preparation of a membrane.

Fabrication of MMMs

MMMs that contained Cu-MOFs were prepared by dispersing the appropriate amount of Cu-MOF powder in 20 wt % POZ in ethanol and 5 wt % PEBAX in 7:3 (w/w) ethanol:water solution. Bulk powder Cu-MOFs were ground using a mortar before the addition into the polymer solution. Prior to the fabrication of the membranes, the mixture was sonicated to ensure good dispersion. Subsequently, the mixture was coated onto a polysulfone macroporous membrane support (Woongjin Chemical Industries, Seoul, Korea) at a rate of ca. 0.025 m s^{-1} using an RK Control Coater (model 101, Control Coater RK Print-Coat Instrumentals, UK) with black bar (wet film deposition thickness of ca. 40 μm). The average thickness of the selective layer was approximately 3.5 μm for POZ and 2 μm for PEBAX. The average pore size of the surface of the polysulfone macroporous membrane support was 0.1 μm, in the asymmetric structure. After the solvent was evaporated in a convection oven at room temperature, the MMMs were dried in a vacuum oven for one day at room temperature.

Characterization

X-ray diffractometer (XRD) patterns were collected at room temperature using a Rigaku X-ray diffractometer equipped with a Cu Kα radiation source ($\lambda = 0.154$ nm). Membrane cross-sections were obtained by fracturing dry membranes under liquid nitrogen and analyzed with a field emission scanning electron microscope (FE-SEM, HITACHI S-4700). Platinum was coated on the samples at 15 nm thickness. Differential Scanning Calorimetry (DSC) thermograms of the MMM were obtained by DSC 8000, Perkin Elmer (USA). The temperature range was −80∼230°C at a heating rate of 15°C/min in a nitrogen atmosphere. The membrane area, 2.25 cm^2, was evaluated using a mass flow meter[30] at pressures of 207 kPa for the membranes. More than three samples were prepared for each concentration of Cu-MOF in the MMMs, and the reported data represent the averaged values for the samples showing CO_2/N_2 selectivity. The unit of permeance is GPU [10^{-6} cm^3 (STP)/(cm^2 s cmHg)], and the ideal selectivity was calculated as the ratio of permeance.

Computational Method

The electronic energies and structures of the stationary species of interest in the gas phase were calculated by full optimization without any geometrical constraints using the density functional

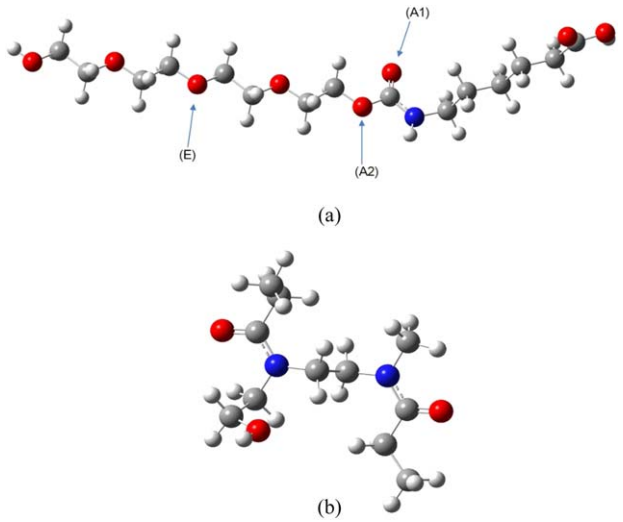

Figure 1. Optimized structure of a simple model of (a) PEBAX and (b) POZ (the arrow represents the approaching direction of CO_2). [Color figure can be viewed in the online issue, which is available at wileyonlinelibrary.com.]

theory method with Gaussian 09 software, using the B3LYP hybrid exchange function[31,32] with a 6-31+G(d,p) basis set.[33] The nature of all stationary point species was verified by calculating their vibrational frequency.[34,35]

RESULTS AND DISCUSSION

Complexation of CO_2 In Modeled Polymer

In general, the gas transport through the PEBAX and POZ membranes obeys a solution-diffusion mechanism. Because the solubility in the polymer matrix depends on the chemical interactions between CO_2 and polar groups of the matrix polymer, the interaction between CO_2 and the matrix were investigated by theoretical approaches using the model of PEBAX and POZ, which are shown in Figure 1. PEBAX is a combination of a nylon 6 segment with polyether segment according to the weight mole fraction, and POZ was structured as a dimer of oxazoline. The four possible configurations of PEBAX were optimized, and the most stable configuration is shown in Figure 1 along with that of POZ.

For PEBAX···CO_2, six initial configurations were constructed for geometric optimization as marked in Figure 1(a). In each of the configurations, the CO_2 molecule was placed at a different location: horizontally and vertically to the plain, which formed with the amide or ether group). The optimized structures in each location are shown in Figure 2.

The formation of these complexes is diffusion-controlled without an activation energy. The B3LYP structure of POZ···CO_2 was obtained with a similar method, and the optimized structures are shown in Figure 2(d).

In the complex with PEBAX, the most stable PEBAX···CO_2 complex is shown in Figure 2(a), in which the CO_2 is located such that it is almost equidistant from the carbonyl oxygen atoms of the amide group in PEBAX. The distance between the C of CO_2 and O of carbonyl is 0.289 nm, and the charge of oxygen is calculated by natural population analyses (NPA),[36,37] the charge densities of the oxygen of carbonyl group increased with the addition of CO_2 from −0.664 to −0.685 by the complexation formation. For the PEBAX···CO_2 complex in which CO_2 was attached to the ether oxygen [Figure 2(c)], the distance between the C of CO_2 and O of ether is 0.341 nm, and the charge of the ether oxygen slightly changed from 0.604 to 0.611. Additionally, the oxygen atoms of the CO_2 molecule are bent outwards to reduce the repulsive interaction with the electronegative oxygen, and it is more significant for CO_2 complexed with carbonyl oxygen. Similar principles influence the structure of the POZ···CO_2 complex, as shown in Figure 2(d).

When compared between the complex formed in the amide region [Figure 2(a)] and the ether region [Figure 2(c)], the distance between the C of CO_2 and O of the polymer in [Figure 2(a)] is shorter than that in [Figure 2(c)]. This implies that the interaction of C and O of the amide is higher than the interaction of C and O of the ether.

The complexation energy (ΔE_c) is defined as the difference between the energy of the matrix···CO_2 complex and the sum

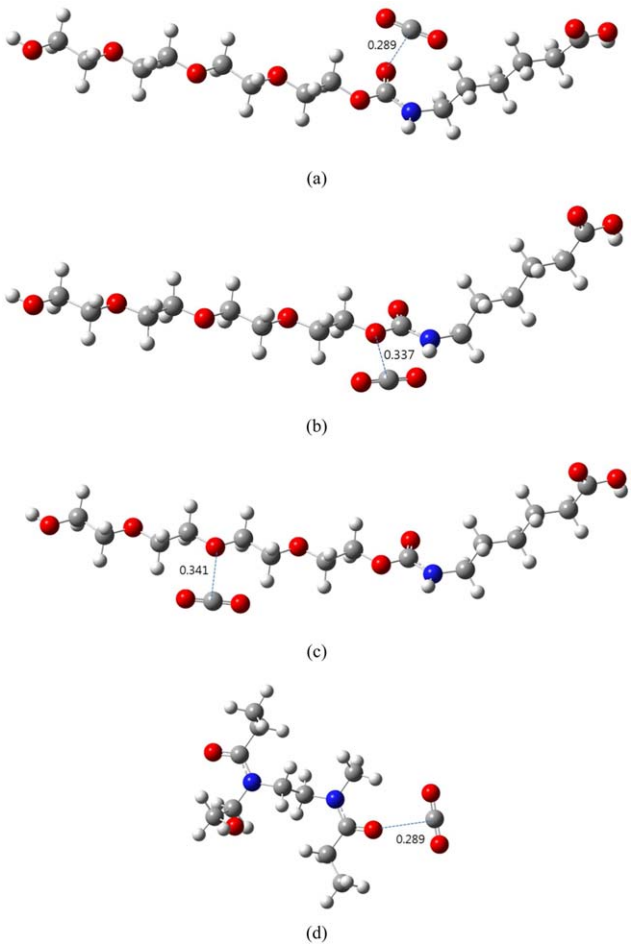

Figure 2. Optimized structure of complexes with CO_2: (a) PEBAX (A1)···CO_2, (b) PEBAX (A2)···CO_2, and (c) PEBAX (E)···CO_2, (d) POZ ···CO_2. [Color figure can be viewed in the online issue, which is available at wileyonlinelibrary.com.]

Table I. Data Obtained from Optimized Geometries of CO_2-Polymer Model Complexes

	Sample ID in Figure 2	ΔE_c (kJ/mol)	D (nm)	$<CO_2$ (°)
PEBAX	(a)	−9.92	0.289	177.5
	(b)	−7.63	0.337	179.2
	(c)	−4.54	0.340	179.0
POZ	(d)	−9.51	0.289	177.4

of the energies of the separate model matrices and CO_2 species. Although it is known that a calculation with a basis set superposition error correction carried out by the counterpoise method of Boys-Bernardi[38] provides a more consistent result with experimental data for the non-covalently bound complexes,[39] our objective is to see the trend in this simplified model; therefore, we only considered the uncorrected ΔE_c between the molecules in this research.

The complexation energies in the gas phase are all negative, as shown in Table I, indicating that their formation is favorable. The ΔE_c values were found to be −9.51 kJ/mol for POZ···CO_2, and the ΔE_c values were −9.92 and −4.54 kJ/mol for amide···CO_2 and ether···CO_2 complexes in PEBAX, respectively, in gas phase. The formation in the gas phase of amide···CO_2 is more favorable than that of ether···CO_2 in PEBAX. The energy and structure of the amide oxygen of the POZ···CO_2 complex are consistent with that in PEBAX.

Considering the relationship between the free energy and the solubility, the polyamide segment would contribute more to the CO_2 solubility than ether segment. However, PEBAX has both rubbery polyether domains and glassy polyamide domains, and most of the gas transport occurs through the rubbery domains; therefore, the sorption contribution of the glassy amide domain is considered to be negligible due to the crystallinity of the amide domains in permselectivity of PEBAX matrix.[22]

Characteristics of MMM Containing Cu-Mof

The formulation of Cu-MOF is $[\{Cu_2(Glu)_2(\mu\text{-bpa})\}\cdot(CH_3CN)]_n$ where Cu_2 units are connected by glutamates (Glu) and 1,2-bis(4-pyridyl)ethane (bpa) ligands. A single-crystal X-ray study revealed that the Cu-MOFs contain Cu_2 dinuclear units connected by Glu to form two-dimensional sheets, and these sheets are bridged by bpa ligands to form the infinite 3-dimensional framework Cu-MOF.[16] The N_2 and CO_2 gas sorption analysis for Cu-MOF has previously been reported.[16] Cu-MOF sorbed 12.7 $cm^3\ g^{-1}$ of CO_2 at 298 K, while no significant sorption of N_2 was observed for Cu-MOF at 298 or even 77 K, showing the effective CO_2 adsorption of Cu-MOF.[16,20] This selective CO_2 sorption of Cu-MOF is known to be based on the different polarizabilities of CO_2 and N_2[16] and implies the possibility of CO_2 carriers for a facilitated transport membrane. Therefore, the intrinsic Cu-MOF selectivity of the CO_2/N_2 is assumed to be high, which implies that Cu-MOF can be utilized as a carrier for CO_2 separation.[20]

The MMM was prepared by casting the Cu-MOF/polymer solution onto a commercial macroporous polysulfone membrane support. The amount of Cu-MOFs in polymer was checked after dissolving the Cu-MOF/polymer film, and the morphology of Cu-MOFs was maintained during the fabrication of the membrane, which was confirmed by XRD.

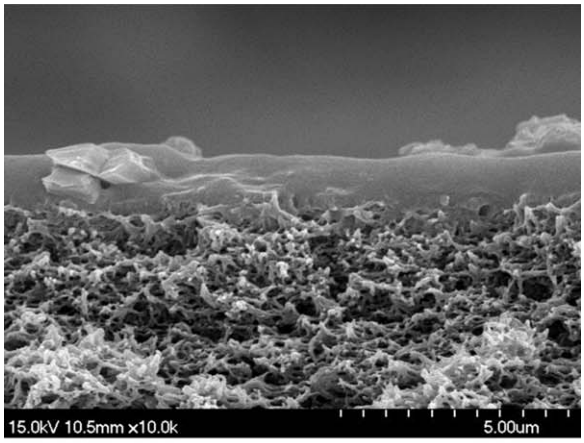

(a)

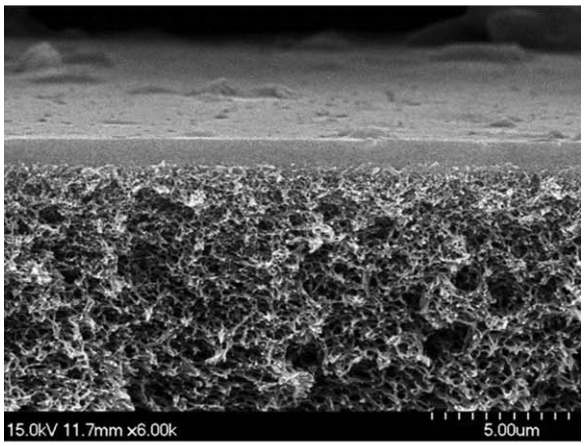

(b)

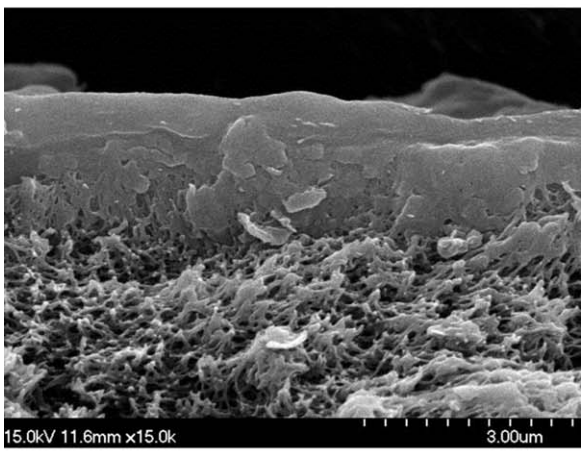

(c)

Figure 3. FESEM images of the cross section of a composite membrane with a selective layer that contains (a) 1.7 (b) 4.8 and (c) 7.2 wt % Cu-MOF in a PEBAX matrix, respectively.

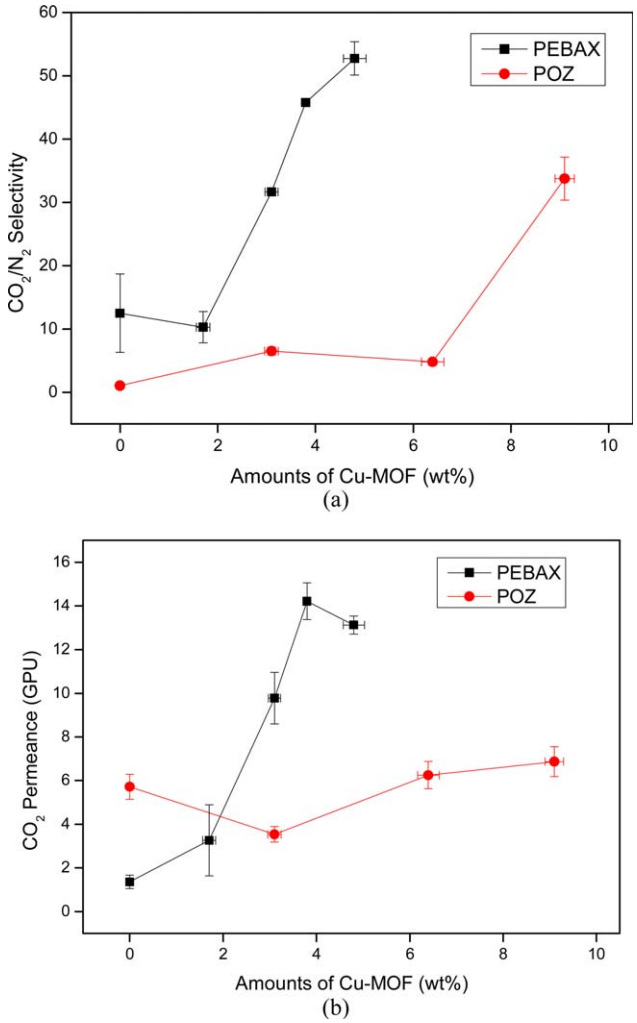

Figure 4. (a) Ideal selectivity and (b) CO_2 permeance of Cu-MOF/PEBAX and Cu-MOF/POZ composite asymmetric membranes with different amounts of Cu-MOF. [Color figure can be viewed in the online issue, which is available at wileyonlinelibrary.com.]

Figure 3 shows the cross-sectional morphology of a composite membrane with a selective layer, which contains different amount of Cu-MOF in PEBAX matrix. The membranes are underlaid by a porous sub-layer with macrovoids, which act only as a mechanical support for the selective layer.

Membrane Performance

The separation performance of the Cu-MOF/PEBAX and Cu-MOF/POZ composite asymmetric membranes, prepared with different amounts of Cu-MOFs, was evaluated. The ideal selectivity of CO_2/N_2 and CO_2 permeances with increasing amounts of Cu-MOFs are shown in Figure 4(a,b), respectively.

The ideal selectivity of CO_2/N_2 was approximately 12.5 and 1.1 for pristine PEBAX and POZ asymmetric membranes, respectively. These values for both pristine membranes are lower than those of the reference,[40] which is probably due to the preparation method using ethanol for the fabrication of the membrane (*vide infra*). The ideal selectivity of CO_2/N_2 for all of the MMMs that contained Cu-MOFs improved, with a greater increase observed in the MMM based in PEBAX than in POZ. For the sample containing more than 5 wt % and 10 wt % loading of Cu-MOFs in PEBAX and POZ matrix, respectively, the ideal selectivity decreased for both MMMs without reproducibility. This decreased selectivity of the membrane with high Cu-MOF loading for MMM implies a non-selective void formation at the interfaces between the Cu-MOFs and the polymer matrix. That is, the Cu-MOF dispersion is probably maximized and beyond the point at which agglomeration of Cu-MOFs becomes significant, resulting in unselective void formations.

In general, MOF loadings in the MMM increased the permeability, resulting in increased permeance at the expense of selectivity.[17,41–45] However, the membranes that contained the Cu-MOF prepared in this study exhibited a significantly increased CO_2/N_2 selectivity while the permeance was maintained (or slightly improved). Because the pore size of Cu-MOF is 0.54 nm $\times$ 0.41 nm, no size or shape selectivity of Cu-MOF is expected, given that the kinetic sizes of CO_2 and N_2 are 0.33 and 0.36 nm, respectively.[16,20] It can be seen that the competitive adsorption of CO_2 over N_2 of Cu-MOF for CO_2 would increase the solubility of CO_2 in the membrane.

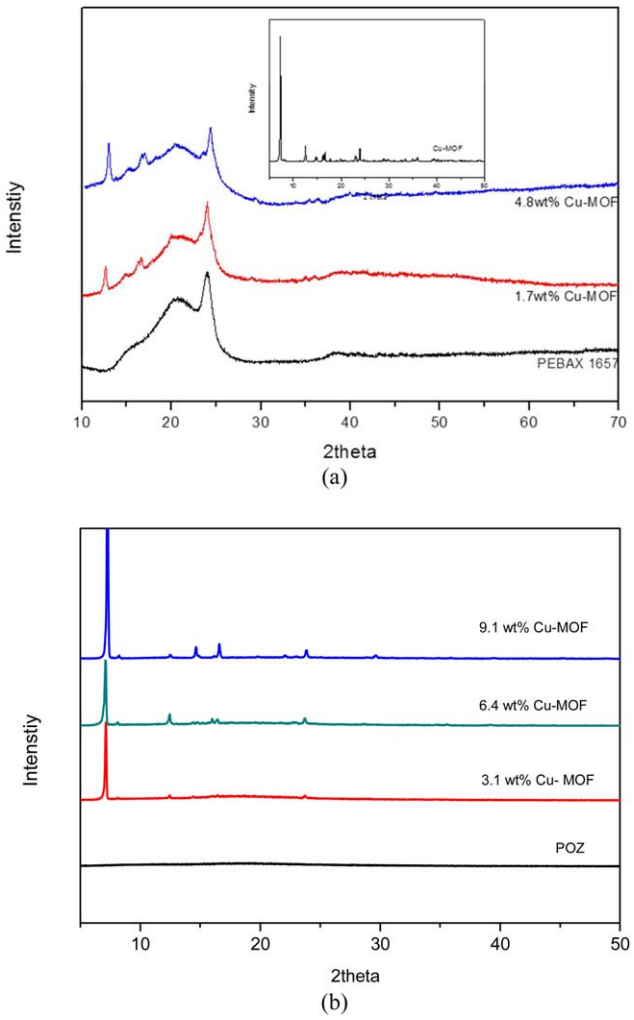

Figure 5. WAXD curves for (a) Cu-MOF/PEBAX and (b) Cu-MOF/POZ film with different amounts of Cu-MOF. [Color figure can be viewed in the online issue, which is available at wileyonlinelibrary.com.]

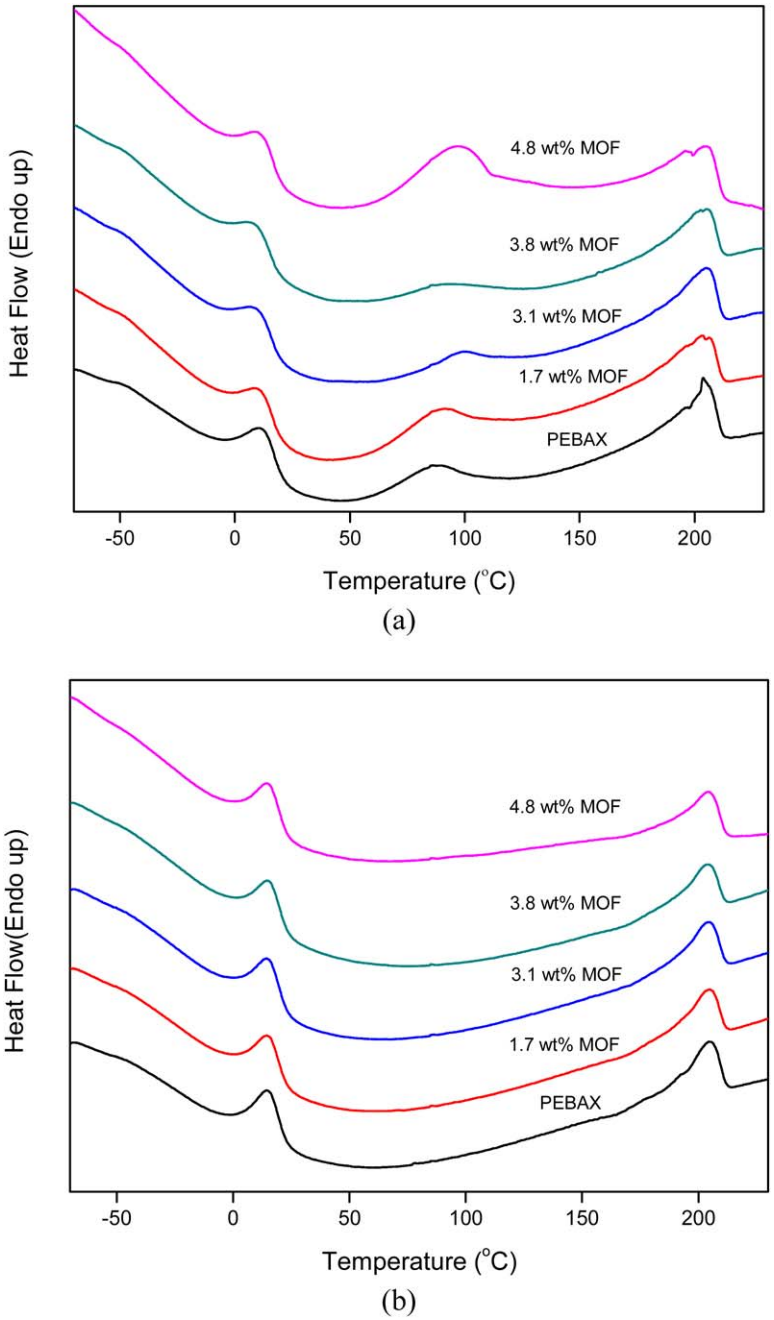

Figure 6. DSC thermograms of Cu-MOF/PEBAX samples with different amounts of Cu-MOF during the (a) first heating and (b) second heating run. Curves are shifted vertically for clarity. [Color figure can be viewed in the online issue, which is available at wileyonlinelibrary.com.]

If we considered the role of the matrix polymer is to disperse Cu-MOFs well enough to perform as a carrier for CO_2-facilitated transport, the increasing amount of CO_2/N_2 ideal selectivity has to be similar. However, we found that the increment of the selectivity is higher for an MMM based on PEBAX than that based on POZ.

Effect of Cu-MOFs on Different Matrices

Figure 5 shows the XRD patterns of the Cu-MOF/polymer matrix film. The insert in Figure 5(a) shows the powder X-ray diffraction pattern of the Cu-MOF. Although some extraneous peaks are observed as the amount of Cu-MOF increased in the sample, the intensities of the peaks of Cu-MOFs increase with increasing Cu-MOF for both MMM based in PEBAX and POZ, indicating that most of the Cu-MOFs maintain their original structure.[20]

The *d*-spacing between polymer chains, which is related to the free volume, was determined because the chain mobility of the polymer matrix could affect the diffusion of gases for our system. PEBAX is a semicrystalline polymer that shows diffraction peaks at 20° and 24° of 2θ, which corresponds to *d*-spacings of 0.44 and 0.37 nm, and these are maintained with the addition of Cu-MOF. On the other hand, the *d*-spacing of a pristine POZ film was estimated to be 0.47 nm, and it decreased to be

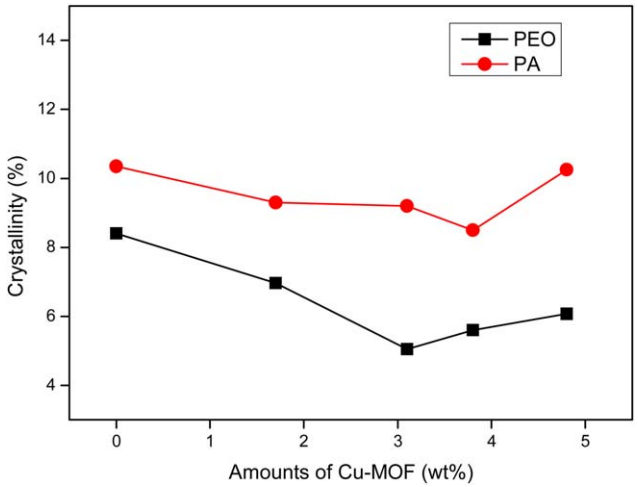

Figure 7. Crystallinity changes with the addition of Cu-MOF in PEBAX matrix. [Color figure can be viewed in the online issue, which is available at wileyonlinelibrary.com.]

0.45 nm with the addition of 9.1 wt % of Cu-MOF and the chain structure of the POZ changed.

The thermal properties of the membranes containing the Cu-MOFs in PEBAX were studied by DSC analysis. The results are displayed in Figure 6(a,b), which are first and second heating run, respectively. DSC provides an excellent tool to assess the miscibility of the Cu-MOFs in PEBAX copolymer because the melting point depression and the reduction in crystallinity is a measure of the strength of the interaction between the polymers and Cu-MOFs.[46] For neat PEBAX in Figure 6(b), two dominant endothermic peaks are present, whose maxima occur at ca. 10 and 210°C. These endotherms can be attributed to fusion of the crystalline fraction of the blocks of poly(ethylene oxide) and polyamide, respectively. In the first heating run as shown in Figure 6(a), there is a very broad ill-defined peak at intermediate temperature. This is probably a kinetically less favorable crystal phase, formed during the fast ethanol evaporation process, which disappears almost completely in the second heating run. This would be the reason why the selectivity of the pristine is lower than that of the reference.

The glass transition temperature decreased from −52.5°C to −53.6°C, which indicates a partial miscibility the Cu-MOF and the PEBAX. The endothermic peak attributed to the crystalline polyamide as well as poly(ethylene oxide) fraction shifts to lower temperature with increasing Cu-MOFs. The weight percent crystallinity in the polyamide block in the copolymer was calculated from the area under the melting peak in DSC results, and the literature value of the enthalpy of fusion for nylon 6 and poly(ethylene oxide) result[40,47] are presented in Figure 7.

The crystallinity of the polyamide block and poly(ethylene oxide) can be estimated as 10.3 and 8.1% in pristine PEBAX film, respectively. The overall crystallinity decreases with increasing Cu-MOFs content, reducing and broadening the peak until approximately 3 wt % of Cu-MOF addition. This indicates an increase in enhancement of an amorphous nature and this will affect the gas permeability as well as the selectivity. With more addition of Cu-MOF, both segmental crystallinities increased, and this could be the reason why the CO_2 permeance decreased with the addition of 4.8 wt % of Cu-MOF in PEBAX.

It is generally known that block copolymers have a different gas permeation behavior from that of homopolymers. The gas permeability is the product of a thermodynamic parameter, the solubility coefficient, and a kinetic parameter, the diffusivity. The solubility depends on the chemical interaction, and rubbers are generally more permeable than glassy polymers. The diffusivity is related to the mobility of the polymer chains and to their packing density or free volume, which allow the passage of the permeant molecules. The crystalline amide block in PEBAX acts as an impermeable phase, which decreases the diffusivity and the permeability. Although the interaction with CO_2 is higher, it lacks sorption sites, whereas ether block in PEBAX acts as the permeable rubbery phase due to its high chain mobility and reasonable interaction with CO_2.[40]

In MMM containing CO_2-selective Cu-MOF, the total CO_2 transport is represented by summation of the Cu-MOF-mediated transport because of the reversible and competitive adsorption of Cu-MOF with CO_2 and Fickian transport through the polymer matrix. With the addition of Cu-MOFs in the polymer matrix, the amount of impermeable polyamide regions in the block copolymer decreases, whereas the high interaction between polyamide and CO_2 has an additive effect on the gas solubility. In addition to the increased rubbery ether block, both of the favorable interaction enhancements of polar ether and amide oxygen with CO_2 result in high solubility selectivity of CO_2 with the addition of Cu-MOF over nonpolar gases. In summary, improvement in the CO_2/N_2 selectivity of a Cu-MOF/PEBAX MMM was achieved via facilitated transport by the CO_2-selective Cu-MOFs due to both an adsorption selectivity of CO_2 over N_2 and the decreased crystallinity of PEBAX in the presence of the Cu-MOFs, which would provide a synergic effect on the CO_2 separation.

CONCLUSIONS

We report the room-temperature preparation of asymmetric MMMs that contain CO_2-selective Cu-MOFs in two different matrices and the characterization the CO_2 permselectivity of the membrane. The preparation method used in this study suggests the possible development of MMMs that contain MOFs for gas separation by tailoring the selective interaction with CO_2.

The homopolymer POZ and the elastomeric block copolymer PEBAX were used as a base polymer matrix and showed the different contribution of CO_2 selectivity by the incorporation of the CO_2-selective MOFs. Both MMMs in the present work show a high CO_2/N_2 selectivity while maintaining the CO_2 permeance with the addition of CO_2–selective Cu-MOFs. XRD, DSC data, and theoretical calculations of the complexation provide valuable physical insights as to the origin of the selectivity enhancement in the membranes. The Cu-MOFs cause a progressive decrease of the overall melting enthalpy of the polyamide as well as poly(ethylene oxide) segment in PEBAX and crystallinity phase of the polyether blocks.

For both MMMs, the reversible affinity of the Cu-MOF for CO_2 primarily contributes to the CO_2/N_2 selectivity, and the higher

permselectivity of MMM based in PEBAX is generally attributed to the extra solubility of CO_2 in the amorphous poly(ethylene oxide) and polyamide phases with the addition of Cu-MOFs. This higher CO_2/N_2 selectivity and CO_2 permeance of the Cu-MOF MMM is due to the competitive adsorption of the two gases onto the Cu-MOF and/or the increase of the amorphous segment in PEBAX.

ACKNOWLEDGMENTS

This work was supported by a Korea CCS R&D Center (KCRC) grant funded by the Korea government (Ministry of Science, ICT & Future Planning) (no. NRF-2014M1A8A1049313) and by the Energy Efficiency & Resources Core Technology Program of the Korea Institute of Energy Technology Evaluation and Planning (KETEP), granted financial resource from the Ministry of Trade, Industry & Energy, Republic of Korea (20140438).

REFERENCES

1. Koros, W. J.; Mahajan, R. J. *J. Membr. Sci.* **2000**, *175*, 181.
2. Freeman, B. D. *Macromolecules* **1999**, *32*, 375.
3. Suzuku, T.; Yamada, Y. *J. Appl. Polym. Sci.* **2013**, *127*, 316.
4. Yu, X.; Zhang, Z.; Rao, H.; Liu, F. *J. Appl. Polym. Sci.* **2012**, *128*, 2823.
5. Robeson, L. M. *J. Membr. Sci.* **1991**, *62*, 165.
6. Bae, T.; Lee, J. S.; Qiu, W.; Koros, W. J.; Jones, C. W.; Nair, S. *Angew. Chem. Int. Ed.* **2010**, *49*, 9863.
7. Zornoza, B.; Martinez-Joaristi, A.; Serra-Grespo, P.; Tellez, C.; Coronas, J.; Gascon, J.; Kapteijin, F. *Chem. Commun.* **2011**, *47*, 9522.
8. Zornoza, B.; Tellez, C.; Coronas, J.; Gascon, J.; Kapteijn, F. *Microporous Mesoporous Mater.* **2013**, *166*, 67.
9. Gascon, J.; Kapteijn, F.; Zornoza, B.; Sebastian, V.; Casado, C.; Coronas, J. *Chem. Mater.* **2012**, *24*, 2829.
10. Couck, S.; Denayer, J. F. M.; Baron, G. V.; Remy, T.; Gascon, J.; Kapteijn, F. *J. Am. Chem. Soc.* **2009**, *131*, 6326.
11. Rodenas, T.; Dalen, M. V.; Garcia-Perez, E.; Serra-Crespo, P.; Zornoza, B.; Kapteijn, F.; Gascon, J. *Adv. Funct. Mater.* **2014**, *24*, 249.
12. Rodenas, T.; Dalen, M. V.; Serra-Crespo, P.; Kapteijn, F.; Gascon, J. *Microporous Mesoporous Mater.* **2014**, *192*, 35.
13. Sumida, K.; Rogow, D. L.; Mason, J. A.; McDonald, T. M.; Bloch, E. D.; Herm, Z. R.; Bae, T.; Long., J. R. *Chem. Rev.* **2012**, *122*, 724.
14. Basu, S.; Cano-Odena, A.; Vankelecom, I. F. J. *J. Membr. Sci.* **2010**, *362*, 478.
15. Won, J.; Seo, J. S.; Kim, J. H.; Kim, H. S.; Kang, Y. S.; Kim, S.; Kim, Y.; Jegal, J. *Adv. Mater.* **2005**, *17*, 80.
16. Hwang, I. H.; Bae, J. M.; Kim, W.; Jo, Y. D.; Kim, C.; Kim, Y.; Kim, S.; Huh, S. *Dalton Trans.* **2012**, *41*, 12759.
17. Huang, A.; Wang, N.; Kong, C.; Caro, J. *Angew. Chem. Int. Ed.* **2012**, *51*, 10551.
18. Shahid, S.; Nijmeijer, K.; Nehache, S.; Vankelecom, I.; Deratani, A.; Quemener, D. *J. Membr. Sci.* **2015**, *492*, 21.
19. Zhang, C.; Dai, Y.; Johnson, J. R.; Karvan, O.; Koros, W. J. *J. Membr. Sci.* **2012**, *389*, 34.
20. Lim, S. Y.; Choi, J.; Kim, H. Y.; Kim, Y.; Kim, S. J.; Kang, Y. S.; Won, J. *J. Membr. Sci.* **2014**, *467*, 67.
21. Bondar, V. I.; Freeman, B. D.; Pinnau, I. *J. Polym. Sci., Part B: Polym. Phys.* **1999**, *37*, 2463.
22. Bondar, V. I.; Freeman, B. D.; Pinnau, I. *J. Polym. Sci., Part B: Polym. Phys.* **2000**, *38*, 2051.
23. Seddigh, M. A. E.; Sani, E. S.; Mohebbi-Kalhori, D. *Chinese J. Polym. Sci.* **2014**, *32*, 402.
24. Murali, R. S.; Sridhar, S.; Sankarshana, T.; Ravikumar, Y. V. L. *Ind. Eng. Chem. Res.* **2010**, *49*, 6530.
25. Yu, B.; Cong, H.; Li, Z.; Tang, J.; Zhao, X. S. *J. Appl. Polym. Sci.* **2013**, *130*, 2867.
26. Messaoud, S. B.; Takagaki, A.; Sugawara, T.; Kikuchi, R.; Oyama, S. T. *Sep. Purif. Technol.* **2015**, *148*, 38.
27. Rabiee, H.; Alsadat, S. M.; Soltanieh, M.; Mousavi, S. A.; Ghadimi, A. *J. Ind. Eng. Chem.* **2015**, *27*, 223.
28. Hohenberg, P.; Kohn, W. *Phys. Rev.* **1964**, *136*, B864.
29. Kohn, W.; Sham, L. *J. Phys. Rev.* **1965**, *140*, A1133.
30. Chae, I. S.; Kang, S. W.; Park, J. Y.; Lee, Y.; Lee, J. H.; Won, J.; Kang, Y. S. *Angew. Chem. Int. Ed.* **2011**, *50*, 2982.
31. Becke, A. D. *J. Chem. Phys.* **1993**, *98*, 5648.
32. Lee, C.; Yang, W.; Parr, R. G. *Phys. Rev.* **1988**, *37*, 785.
33. Hehre, W. J.; Radom, L.; Scchleyer, P. V.; Pople, J., Eds. *Ab initio* Molecular Orbital Theory; John Wiley & Sons: New York, **1986**.
34. Pople, J. A.; Krishnan, R.; Schlegel, H. B.; Binkley, J. S. *Int. J. Quantum Chem.* **1979**, *13*, 225.
35. Pople, J. A.; Schlegel, H. B.; Krishnan, R.; Defrees, D. J.; Binkley, J. S.; Frisch, M. J.; Whiteside, R. A.; Hout, R. F.; Hehre, W. J. *Int. J. Quantum Chem.* **1980**, *15*, 269.
36. Reed, A. E.; Weinhold, F. *J. Chem. Phys.* **1983**, *78*, 4066.
37. Reed, A. E.; Weinstock, R. B.; Weinhold, F. *J. Chem. Phys.* **1985**, *83*, 735.
38. Deverell, C.; Morgan, R. E.; Strange, J. H. *Mol. Phys.* **1970**, *18*, 553.
39. Steckel, J. A. *J. Phys. Chem. A.* **2012**, *116*, 11643.
40. Kim, J. H.; Ha, S. Y.; Lee, Y. M. *J. Membr. Sci.* **2001**, *190*, 179.
41. Li, Y.; Liang, F.; Bux, H.; Feldhoff, A.; Yang, W.; Caro, J. *Angew. Chem. Int. Ed.* **2010**, *49*, 548.
42. Thompson, J. A.; Chapman, K. W.; Koros, W. J.; Jones, C. W.; Nair, S. *Microporous Mesoporous Mater.* **2012**, *158*, 292.
43. Brown, A. J.; Johnson, J. R.; Lydon, M. E.; Koros, W. J.; Jones, C. W.; Nair, S. *Angew. Chem. Int. Ed.* **2012**, *51*, 10615.
44. Huang, A.; Bux, H.; Steinbach, F.; Caro, J. *Angew. Chem. Int. Ed.* **2010**, *49*, 4958.
45. Kwon, H. T.; Jeong, H. *J Am. Chem. Soc.* **2013**, *135*, 10763.
46. Bernardo, P.; Jansen, J. C.; Bazzarelli, F.; Tasselli, F.; Fuoco, A.; Friess, K.; Izak, P.; Jarmarova, V.; Kacirkova, M.; Clarizia, G. *Sep. Purif. Technol.* **2012**, *97*, 73.
47. Yifan, L.; Wang, S.; Wu, H.; Wang, J.; Jiang, Z. *J. Mater. Chem.* **2012**, *22*, 19617.